

# Full-Spectrum, Angle-Resolved Reflectance and Transmittance of Optical Coatings Using the LAMBDA 1050+ UV/VIS/NIR Spectrophotometer with the ARTA Accessory

## UV/Vis/NIR Spectroscopy

### Authors:

Zhengshan Yu  
Dr. Zachary Holman  
School of Electrical, Computer,  
and Energy Engineering  
Arizona State University  
Tempe, AZ

Mark O'Neill  
3M Renewable  
Energy Division  
St. Paul, MN

Christopher Lynch  
PerkinElmer, Inc.  
Shelton, CT

### Introduction

Optical coatings composed of thin films of dielectric materials have long been commonplace in both the optics and glass industries. For instance, stacks of alternating high- and low-refractive-index layers are used to form Bragg mirrors in laser cavities, and magnesium fluoride layers are used as antireflection coatings on display screens. In the last two decades, however, the range of available optical coatings has broadened considerably as new materials have emerged to meet new applications. These coatings are not necessarily planar or fully dense—leading to light scattering—and they may be intended to function at non-normal angles of incidence, for which *s*- and *p*-polarized light behave differently. The solar energy industry provides several nice examples: zinc oxide coatings grown by chemical vapor deposition naturally develop a pyramid surface texture that has been employed to scatter light in thin-film solar cells.<sup>1</sup> Holographic filters, formed by patterning the refractive index of a polymer, split the solar spectrum into beams of distinct colors separated in space (much like

a prism), and photovoltaic cells tuned to each wavelength may be placed at these foci to form a new type of multi-junction solar cell.<sup>2</sup> A “coating” of silicon nanocylinders on the front of a silicon solar cell acts as a Mie scatterer that has been shown to reduce reflection—thereby increasing absorption in the solar cell—for a wide range of angles of incidence and polarization.<sup>3</sup>

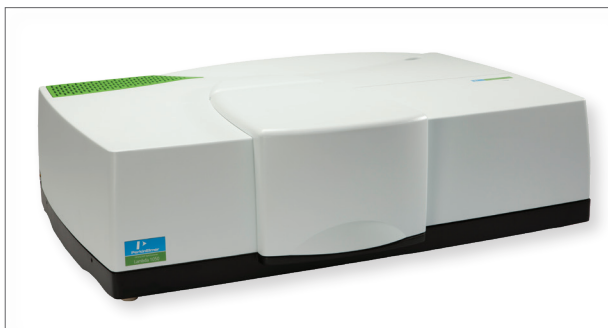


Figure 1. LAMBDA 1050+ High Performance UV/Vis/NIR Spectrophotometer.

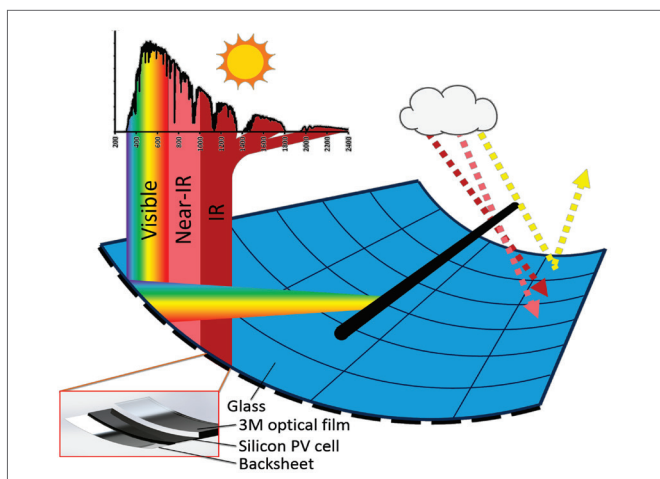


Figure 2. Rendering and schematic of the proposed curved photovoltaic module. The 3M<sup>®</sup> visible mirror film would make the module appear mirrored at visible wavelengths but black at near-infrared wavelengths.

For all optical coatings—and in particular those that receive light from, or direct light into, non-normal angles—it is vital to characterize the wavelength-, angle-, and polarization-resolved reflectance and transmittance. The PerkinElmer Automated Reflectance/Transmittance Analyzer (ARTA) is a drop-in accessory for the LAMBDA 1050+ UV/VIS/NIR spectrophotometer that uses a goniometer to rotate a sample with respect to the beam (varying angle of incidence) and independently rotate an integrating-sphere detector with respect to the sample (varying angle of detection). For any incidence angle/detection angle pairing, spectra may be collected for *s*- and *p*-polarized light in the wavelength range of 250–2500 nm.

The ARTA automatically runs a user-specified table of these measurements, allowing users to efficiently answer the question: “Where does all of the incident light go?”

In this note, we investigate the performance of a long-pass optical film (“visible mirror film”) manufactured by 3M<sup>®</sup>.<sup>4</sup> 3M<sup>®</sup> markets a wide range of these plastic films. They consist of hundreds of layers of transparent polymers of varying thickness and refractive index that together reflect and transmit designated parts of the solar spectrum for applications such as low-emissivity window glass. The visible mirror film chosen for this study absorbs UV light (<350 nm), reflects visible light, and transmits infrared light (>750 nm). We are interested in integrating this film into a curved silicon photovoltaic module, as shown in Figure 2, because the silicon solar cells convert light near their bandgap (700–1100 nm) to electricity with efficiencies exceeding 40%, but shorter wavelengths mostly generate waste heat and are converted with much lower efficiency. By placing the 3M<sup>®</sup> film in front of the solar cells, the infrared wavelengths will be transmitted to the cells while the poorly used shorter wavelengths will be reflected to a focus where another solar collector (photovoltaic, thermal, or chemical) that is tuned to visible light may be placed. The curved photovoltaic module is intended to be placed on a one-axis tracker that will follow the

sun from East to West, but the 3M<sup>®</sup> optical film will still receive sunlight at angles of incidence from 0–60° (in Phoenix, AZ) over the course of the year. Consequently, to determine the annual power output of the entire solar collector, we must first characterize the wavelength-, angle-, and polarization-resolved performance of the 3M<sup>®</sup> optical film.

## Experimental

The PerkinElmer LAMBDA 1050+ UV/VIS/NIR spectrophotometers are dual-beam, dual-monochromator instruments equipped with an optional 150 mm integrating sphere accessory. The high performance coated integrating sphere contains both silicon and InGaAs detectors so that accurate spectra may be collected from 200–2500 nm. The total reflectance, total transmittance, diffuse reflectance, and diffuse transmittance of a film, substrate, or liquid (in a cuvette) may be measured by positioning the sample at either the entrance or exit port of the integrating sphere, and removing the specular port in the case of diffuse measurements. For more detailed analysis of the angular dependence of reflection and transmission for arbitrary angle of incidence, the integrating sphere accessory may be exchanged with the ARTA accessory (Figure 3) in approximately 10 minutes. The ARTA also utilizes a (60 mm) integrating sphere with PMT and InGaAs detectors, but this sphere is mounted on a goniometer so that it may circle 340° around the sample in the horizontal plane, collecting light that falls within its adjustable-width entrance aperture. The sample, which again may be a film, substrate, or liquid, is also mounted on the goniometer and allowed to rotate—independent of the detector—so that a user may choose arbitrary angles of incidence (with respect to the fixed source) and detection. Control of the ARTA is integrated into the UV Winlab software so that a user can specify a run table that will automatically execute.

In the present experiments, total and angular-resolved reflectance and transmittance spectra of a 3M<sup>®</sup> visible mirror film were collected using a LAMBDA 1050+ spectrophotometer. For the total reflectance and transmittance spectra, the film was placed at the entrance (0° angle of incidence) or exit (8° angle of incidence) of the 150 mm integrating sphere accessory and spectra were collected over 250–2500 nm using unpolarized light. For the angular-resolved measurements, the film was mounted in the goniometer holder of the ARTA accessory and spectra were collected over 250–2500 nm separately for *s*- and *p*-polarized light (Figure 3). In some measurements, the angle of incidence was varied between 5–85° in 5° increments, and the detector movement was coordinated so that the detector position always corresponded to the specular beam (10° increments). In others, the angle of incidence was fixed while the detector swept a full circle around the sample in 1° increments. The latter experiments were done with slits of varying width placed in front of the detector so as to vary the angular resolution of the measurements.

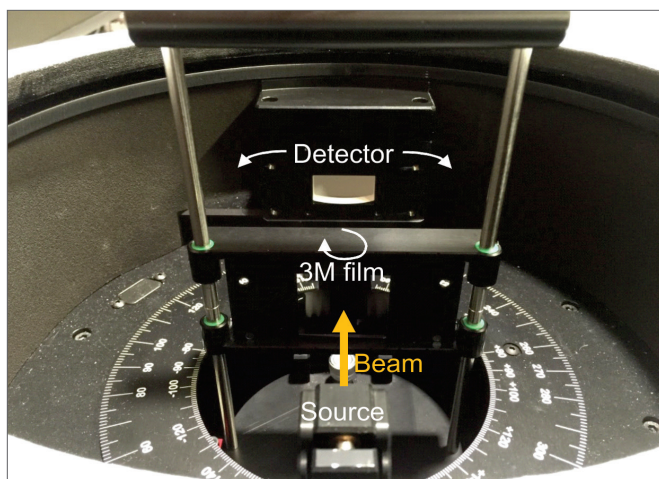


Figure 3. Photograph of the ARTA with the 3M<sup>®</sup> film (which looks like a mirror since it reflects visible wavelengths) mounted in the sample holder. The detector is shown without a slit aperture, which corresponds to an acceptance angle of 20°.

## Results

Before employing the ARTA for in-depth analysis of the 3M<sup>®</sup> film, the total (specular + diffuse) reflectance and transmittance of the free-standing film was measured at nominally normal incidence using the integrating sphere accessory of the LAMBDA 1050+. The results, shown in Figure 4, reveal that the film has the desired sharp transition from reflecting to transmitting at approximately 750 nm, with a visible reflectance of nearly 100% and an infrared transmittance of approximately 90%. This same film was modeled by 3M<sup>®</sup> using the known thicknesses and refractive indices of the constituent polymer layers, and the simulated spectra match the measured spectra to within 2% at most wavelengths.

As the film is planar with low surface roughness, the total reflectance in Figure 4 should be nearly identical to the specular reflectance measured with the ARTA at the same 8° angle of incidence. The specular reflectance resolved by angle of incidence and polarization is displayed in Figure 5 as a contour plot, and, as expected, a horizontal slice taken just above the x-axis looks like the reflectance in Figure 4. Note that the angle of detection was always twice the angle of incidence—i.e., the detection angle associated with the specular beam—for these measurements. For both polarizations, the reflecting-to-transmitting transition remains sharp up to angles of incidence of 50°, but has a slight blue shift. In the intended solar energy conversion application, this will have the effect of shifting over the course of a year the fraction of light coupled to the curved photovoltaic module and to the solar collector at its focus—inconvenient but tolerable with proper engineering. However, for angles of incidence above approximately 50°, the transition dissolves for s-polarized light and the film begins to lose its function as a spectrum splitter. A significant consequence of this is that the curved photovoltaic mirror will work poorly during winter or summer months for latitudes greater than approximately [30°].

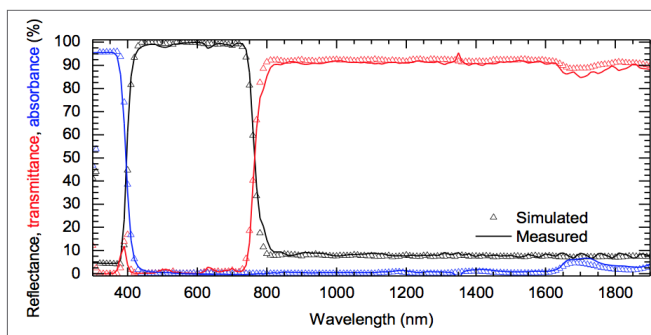


Figure 4. Total reflectance and transmittance spectra of a 3M<sup>®</sup> visible mirror film measured with the 150 mm integrating sphere accessory. Also shown are the simulated spectra calculated by 3M<sup>®</sup>. The absorbance of the film was calculated as 1-R-T.

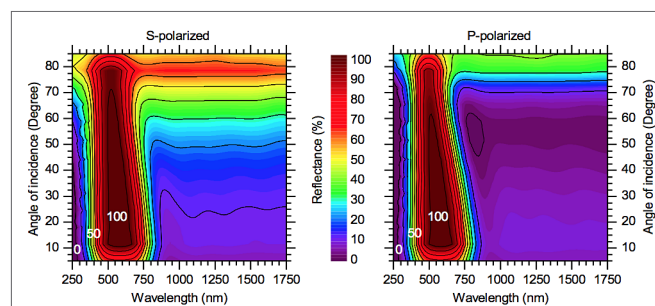


Figure 5. Angle-resolved reflectance spectra of a 3M<sup>®</sup> visible mirror film for s-polarized (left) and p-polarized (right) light. The reflectance color scale is common to both plots. Spectra were measured with the ARTA accessory using 5° steps in the angle of incidence. The detector was rotated at each angle of incidence so as to always receive the specularly reflected beam.

After the optical performance of the free-standing film was characterized, film samples were laminated between silicon wafers and glass substrates using various encapsulants to approximate the final, curved, spectrum-splitting photovoltaic module. Figure 6a is a photograph of three such laminates and indicates that the film may either remain planar or become wrinkled to varying degrees during lamination, depending on the details of the process and the encapsulant used. If the curved photovoltaic module is to concentrate the reflected visible light at its focus, the film must remain planar and conformal with the glass surface. The goniometric nature of the ARTA, coupled with the variable acceptance angle of the detector aperture, allows the angular distribution function of scattered light to be quickly measured in transmission or reflection. Figure 6b-d which appear on the next page, displays such data for two laminates—one visibly planar and the other visibly lightly wrinkled—as well as a free-standing film. 600 nm light, which is in the middle of the reflected band, was used for all samples; the free-standing film was also measured at 1100 nm, where the film transmits, for reference (this was not possible with the laminates because the silicon wafer absorbs this light). To perform these measurements, the angle of incidence was held constant at 30° while the detector automatically circled around the sample. The free-standing film and planar laminate show near-unity reflectance at the specular angle, consistent with Figure 5, even when the detector aperture is closed down to a 5° acceptance angle. That is, all light is reflected within a 2.5°-half-angle cone centered

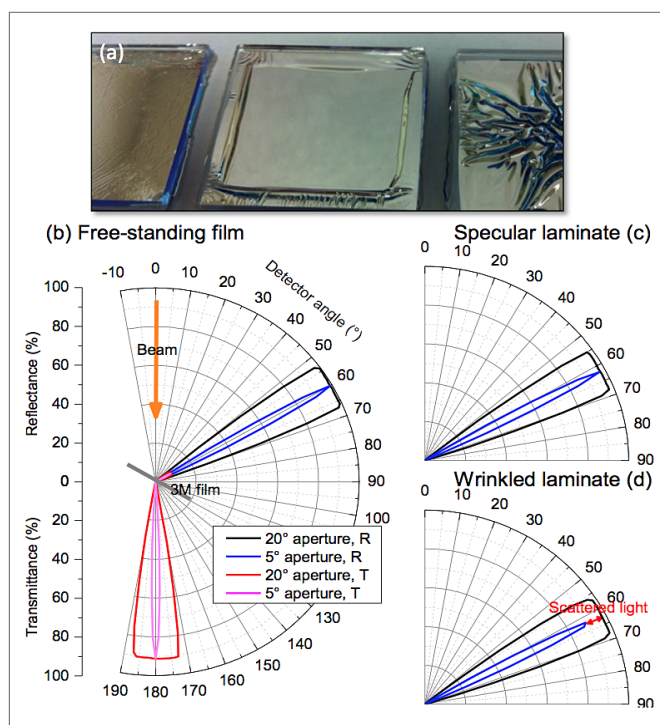


Figure 6. (a) Photograph of three glass/3M<sup>®</sup> film/silicon wafer laminates with different encapsulants. (b) Reflectance and transmittance of the free-standing 3M<sup>®</sup> film as a function of the detector angle. In these polar plots, the radial length of the signal corresponds to the intensity; the outermost circle is 100% reflectance or transmittance. In addition, the beam appears to have a wider spread as the detector aperture is increased because for an, e.g., 20° acceptance angle, all of the light is still detected when the detector is <10° from the specular angle. Reflectance of the (c) visibly specular laminate in the middle of the photograph in (a) and the (d) visibly wrinkled laminated in the left of the photograph in (a).

at the specular angle. The wrinkled sample also reflects all light within a 10°-half-angle cone, but only 89% within a 2.5°-half-angle cone; the wrinkles clearly reduce specularly. The scattered light would miss the focus of the curved photovoltaic module, essentially reducing the concentration of light that arrives at the solar collector placed there.

## Conclusion

We evaluated a 3M<sup>®</sup> visible mirror film for potential use in a new curved photovoltaic module using a LAMBDA 1050+ spectrophotometer with an ARTA accessory. In this application, the 3M<sup>®</sup> film must transmit near-infrared photons to the underlying silicon solar cells (where they will be converted directly to electricity) while reflecting visible photons to the focus of the module where they may be absorbed by, for example a wavelength-agnostic thermal absorber used to drive a heat engine. Angle-resolved reflectance and transmittance measurements with the ARTA indicated that the free-standing 3M<sup>®</sup> film is an effective optical filter for both s- and p-polarization and angles of incidence of up to approximately 50°. To maintain its efficacy when laminated to the curved glass of the proposed module, the film must be conformally attached to the glass (without wrinkles), and ARTA measurements with a narrow detector aperture revealed the degree to which each evaluated lamination procedure produced the desired result. We are presently using the spectra generated by the ARTA to estimate the annual energy output of a power plant employing these curved modules with thermal receivers at their foci, taking into account the daily and annual movement of the sun and the resulting variation in angle of incidence on the module. We are also pursuing optical filters that reflect both visible and infrared light (while transmitting near-infrared light), and the performance of these is under study with both the integrating sphere and ARTA accessories.

## Reference

1. S. Fay, *et al.*, "Opto-electronic properties of rough LP-CVD ZnO : B for use as TCO in thin-film silicon solar cells", *Thin Solid Films* 515, 2007, pp. 8558-8561.
2. N. Mohammad, *et al.*, "Enhancing photovoltaic output power by 3-band spectrum-splitting and concentration using a diffractive micro-optic", *Optics Express* 22, 2014, pp. A1519-A1525.
3. J. V. van de Groep, *et al.*, "Transparent Conducting Silver Nanowire Networks", *Nano Lett* 12, 2012, pp. 3138-3144.
4. M. F. Weber, *et al.*, "Giant birefringent optics in multilayer polymer mirrors", *Science* 287, 2000, pp. 2451-2456.